

Lasers in Manufacturing Conference 2019

# Thermal monitoring of Direct Laser Metal Deposition of a Nickel-based superalloy

Marco Mazzarisi<sup>a\*</sup>, Sabina Luisa Campanelli<sup>a</sup>, Andrea Angelastro<sup>a</sup>, Michele Dassisti<sup>a</sup>,  
Matteo Duraccio<sup>a</sup>, Fania Palano<sup>b</sup>, Antonella Rizzo<sup>b</sup>, Marcello Massaro<sup>b</sup>

<sup>a</sup>*Dept. of Mechanics, Mathematics and Management, Politecnico di Bari, Viale Japigia 182, 70126 Bari, Italy*

<sup>b</sup>*ENEA, Centro Ricerche di Brindisi c/o Cittadella della Ricerca, S.S.7 Appia km 706, 72100 Brindisi, Italy*

---

## Abstract

Additive Manufacturing has been increasingly successful in the industrial and aeronautical sector. The Direct Laser Metal Deposition (DLMD) technology is taking a leading role in the field of coating and repair of components with complex geometries. The process is characterised by high cooling rates that produces extremely fine microstructures with high mechanical properties. The monitoring of process parameters and thermal cycles assumes a key role and determines the quality of the deposition. In this work, an Ytterbium fiber laser source was used to build several single clad depositions of a Nickel-based superalloy powder on a substrate of the same material. Field temperature monitoring was performed using a high frequency (100Hz) IR thermal camera which allowed an accurate monitoring of maximum temperature and thermal cycles. Thermal data and process parameters were compared with metallographic analysis in order to understand the relation between geometrical characteristics and defects of clads.

Keywords: Direct Laser Metal Deposition; IR thermal monitoring; process parameters

---

## 1. Introduction

The Direct Laser Metal Deposition (DLMD) is an innovative technology used to repair and manufacture metal components. The DLMD uses a laser beam focused on the substrate in order to create a melting pool in which the powder is carried by means of an inert gas flow, that is coaxial or lateral to the laser beam, to

---

\* Corresponding author. Tel.: +39-3891263017.  
E-mail address: marco.mazzarisi@poliba.it.

create a thick clad. In this process the designed geometry is obtained layer after layer, through a series of adjacent depositions, as programmed in a tool path compiled by a specific CAM software [Wohlers and Gornet, 2014; Zhong et al., 2004]. Different industrial sectors (aeronautical, automotive and military) are showing a great interest for the technique. It presents several advantages such as versatility in production phase, complex geometries and fine microstructures sporting high mechanical properties. All of them make the process an excellent alternative to the classical subtractive manufacturing [Imran et al., 2011; Peng et al., 2007; Gao et al., 2015]. However, the lack of quality assurance for elements manufactured using Additive Manufacturing is a relevant technological barrier limiting its industrial diffusion. In order to achieve the high-quality standards of the components required by the aeronautical sector, it is necessary to perform an extremely accurate control of the main parameters involved in DLMD [Angelastro et al., 2011]. Researchers are currently studying new devices and integrated adaptive approaches that can monitor the process thus ensuring the final product quality. The most significant variable to monitor is the temperature field, that can be measured by means of contact sensors such as thermocouples or contactless sensors such as pyrometers and thermal imaging systems. Commercial thermocouples showed some issues caused by high contact temperatures, so contactless sensors represent an appropriate choice in this case. Moreover, thermal imaging cameras show advantages over pyrometers, being the first a full-thermal field technique and not a point-to-point technique [Liu et al., 2017]. Several works in the literature analyse the temperature field of metallic powder deposition, indicating the most relevant process parameters and the consequences on deposition clad. Emamian et al., 2017 demonstrated that carbides morphology in a metal matrix strongly depends on pre-heating and cooling rates. They carried on the process monitoring by means of a thermal camera to compute in real time the cooling rate and the evaluate the scan speed influence on it, with the aim of controlling grain morphology and mechanical properties. Farshidianfar et al., 2016a; 2016b employed a thermal camera for recording weld pool temperatures and compute the cooling rate (by means of a suitable algorithm), which is considered the fundamental parameter that influences microstructure and then the overall clad quality. The thermal parameters were defined by the instantaneous heat flux, which depends by several factors such as scan speed, laser power and beam diameter. So, the authors identified some combined indices to assess the clad quality. Muvvala et al., 2017 monitored thermal cycles by means of IR pyrometers and studied the relationship between process parameters, clad geometry and cooling/heating rate. They demonstrated that the main thermal parameter affecting quality is the cooling rate, which in turns depends on scanning rate and laser power. Campanelli et al. 2018 deduced that defectiveness, such as cracks and porosity, strongly depends on peak temperature and cooling rate. By means of an IR thermal camera they monitored the thermal field in DLMD processes for Nickel superalloy powder deposition on stainless steel substrates. Moreover, they examined thermal cycles effects on clad geometry and dilution, particularly considering the importance of pre-heating due to previous depositions on the same sample. Song et al., 2012 designed a hybrid control system including a dual-color pyrometer to measure the melt pool temperature and three high-speed CCD cameras to measure the melt pool height. The device is used to control both height growth and melt pool temperature at each deposition layer modifying laser power input to improve dimensional accuracy. Ya et al., 2016 developed a 2D thermal model of laser cladding process based on mass and energy balance, thus comprising powder efficiency. The melting pool depths and HAZ thicknesses were plotted against the isotherms generated in numerical simulations. The model is able to accurately predict the clad geometry and the thermal cycles during the laser cladding process. DLMD can operate on advanced materials and complex geometries, but for ensuring high quality levels requires a monitoring, control and actuation systems aiming at keeping the process parameters within the optimal ranges. The main objective of the present study is to understand the relationship between the main process parameters and the consequent thermal field for a Nickel-based superalloy. Moreover, the

influence of peak temperature and cooling rate on the geometrical characteristics have been determined to lay the groundwork for a control system.

## 2. Machine setup and materials

Industrial monitoring of thermal parameters such as temperatures and cooling rates should bring to the development of a control system allowing the manufacturer to achieve the desired microstructure and mechanical properties. In Thermographic data detected during the process were subsequently elaborated with specific suitable algorithms implemented in MATLAB in order to identify some thermal parameters representing process efficiency and deposition quality.

### 2.1. DLMD setup

In this work a Nickel-based superalloy powder was deposited on a substrate of the same composition having a thickness of about 6 mm. A 5-axis machine equipped with a deposition head and a coaxial nozzle was used. A fiber laser with a nominal power of 4kW and wavelength of 1.070  $\mu\text{m}$  was employed (YLS 4000 IPG Photonics Ytterbium Laser System). Argon gas was employed as carrier gas for the powder coming from an external powder feeder. The same gas is used as shielding gas to prevent clad oxidation.

### 2.2. Thermographic setup

For monitoring the thermal behavior of the cladding process, a device equipped with a FLIR NIR SC7000 thermal imaging camera featuring a Focal Plane Array cooled detector, a high acquisition speed and 20mK NETD (temperature difference corresponding to the background noise) was used. Altair software has been used for remote data acquisition and processing. The capability of detecting temperatures up to 2500°C is typical of the thermal imaging camera that mounts filtering lenses to evaluate different wavelengths, in order to automatically set the correct lens compliant with the current processes. The thermal imaging camera can suffer damage caused by critical environmental conditions. In this regard, a Plexiglas protection device has been realized and endowed with an IR window in sapphire crystal, transparent to IR radiation. Some thermographic parameters have been appropriately set. For each deposition the acquisition interval was set at 250 seconds. An image acquisition rate of 50 Hz has been set, but the frequency for image elaboration was 5 Hz with an interaction time of 12  $\mu\text{s}$ . It allows us to observe a temperature range between 483 and 2117°C. The choice of the emissivity value of Nickel-based superalloy at high temperatures is one of the problems related to the use of non-contact monitoring. For the experimental calculation of the material emissivity value, the substrate was warmed up to 800°C in an oven and the emissivity values were estimated. The value corresponding to the maximum considered temperature was selected and it was assumed as a constant in the molten pool. In fact, some authors [Emamian et al., 2017; Farshidianfar et al., 2016a] consider the emissivity variation not significant, as long as a constant value is used during the whole process monitoring and in [Farshidianfar et al., 2016a] the authors consider the emissivity referred to powder material. We identified some characteristics points for each deposition, and we decided to monitor the thermal cycles related to:

- Beginning point
- Half point
- End point

We can compare the thermal behavior of the three different points of the sample, that are interested by the laser path and consequently by heating and fusion phenomena at different times. In this way it is possible to evaluate thermal gradients in different points and times and compare them, thus retrieving information about all thermal fields.

### 2.3. Experimental plan

The established experimental plan included the variation of 3 process parameters such as laser power (400 - 600 kW), scanning speed (500 - 1000 mm/min) and powder flow rate (1.5 - 2.5 - 5-10 g/min), while the spot diameter of 1 mm and the gas flow of 3 l/min have been kept constant. The plan adopted is summarized here in the following table:

Table 1. Experimental plan

<i>N</i>	<i>Laser power [W]</i>	<i>Translation speed [mm/min]</i>	<i>Powder flow [g/min]</i>
1	400	500	1,5
2	600	1000	1,5
3	400	500	2,5
4	600	1000	2,5
5	400	500	5
6	600	1000	5
7	400	500	10
8	600	1000	10

The idle time between each deposition of a single track was established in 180 s, in order to allow the cooling of the substrate and to avoid a pre-heating effect that can influence the subsequent depositions. After this cladding phase, the traces were trimmed, then polished and chemically etched. For the analysis of geometry and microstructure, a metallurgical microscope was used with a Nikon Eclipse MA200 digital video camera, optimized for digital imaging.

## 3. Results and discussion

### 3.1. Thermographic analysis

The analysis of thermal cycles was possible thanks to the IR thermal system, which acquired data during the depositions. An optical filter with an integration interval of 12  $\mu$ s was mounted on the camera, capable of capture the temperature range between 483°C and 2117°C.

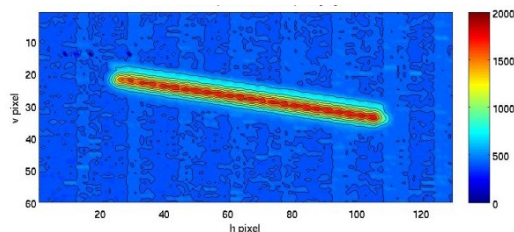


Fig. 1. Thermogram whit isotherms indicating the maximum temperature reached in every point of the deposition path

The thermal videos were analysed using the MATLAB software. Since the thermograms referred to each frame do not present the global information about DMLD process over time, a suitable algorithm was implemented in order to plot, given a fixed setup, a single image reporting the maximum temperatures reached in every timestep. In order to compare the eight depositions, we evaluated the maximum temperature and the different thermal behaviours obtained in each of them (see following graphs).

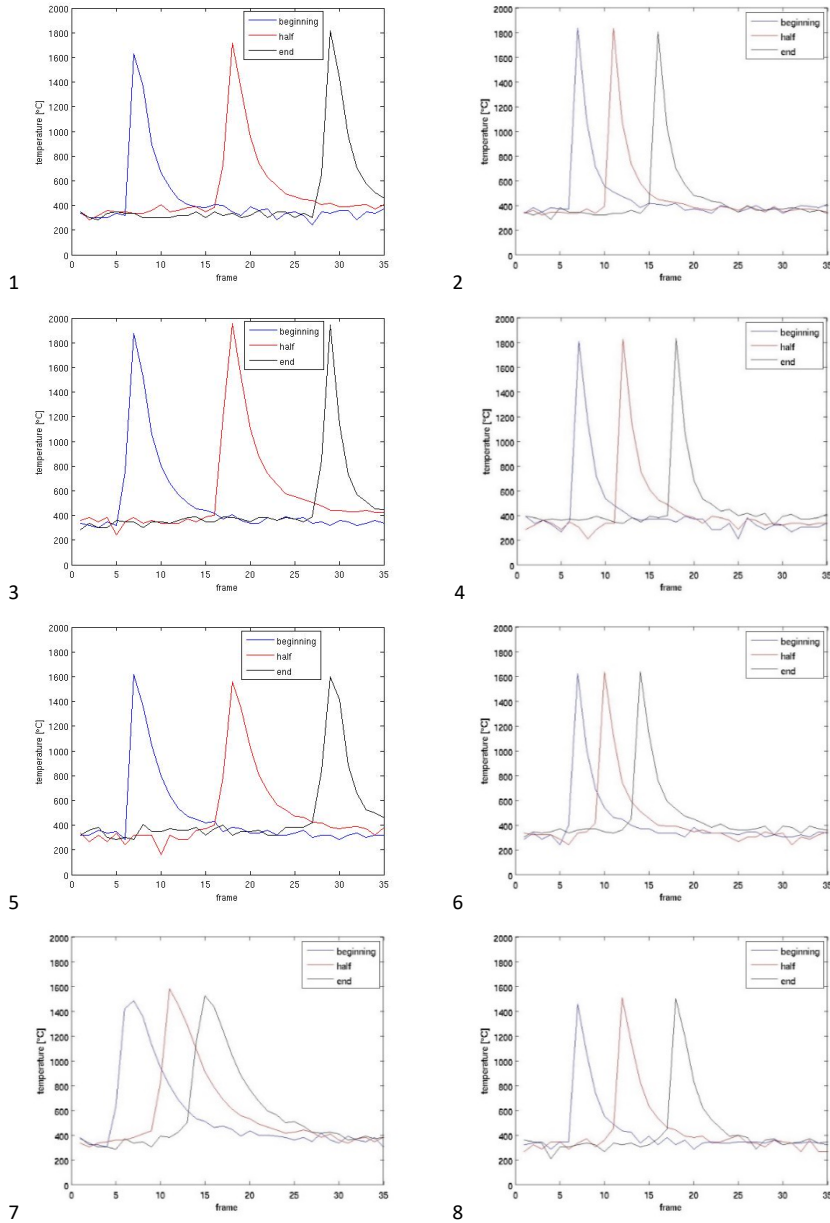


Fig. 2. Comparison between the thermal cycles of different characteristic points for each deposition.

In the graphs (Fig. 2) we marked the melting temperature ( $T_m$ ) of the alloy equal to 1350°C and we immediately notice that all the tracks have reached a complete melting as long as they reach temperatures higher than  $T_m$ . From the graphs we also note that the maximum temperature is reached for low powder flow rates, because in these cases the small quantity of powder does not shield the laser beam. Temperatures dramatically decrease as the powder flow rate increases, and there is a significant difference between 5 g/min and 10 g/min.

During the analysis, three points along the deposition path were chosen to characterize the process and verify the homogeneity of the temperatures during the process: the point corresponding to the deposition beginning, to the centre and to the end of each line. Analysing the collected data, we notice that the temperature peak keeps almost constant for the whole duration of the track as shown in figure 3.a.

For each deposition the cooling rate was calculated at the key points of the track, according to the following formula:

$$\text{Cooling rate} = \frac{T_{\max} - T_{it}}{t(T_{\max}) - t(T_{it})} \quad (1)$$

Where:

- $T_{\max}$  is the maximum temperature reached in a point;
- $T_{it}$  is the interaction temperature equal to 483°C;

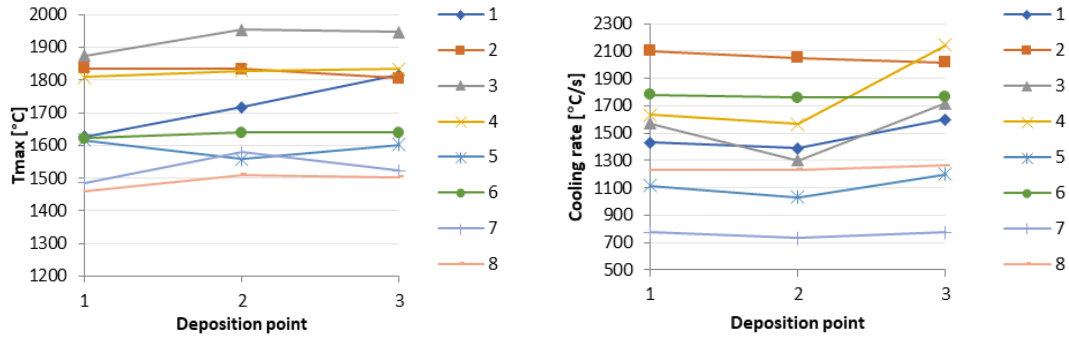


Fig. 3. (a) Trend of maximum temperatures of the characteristic points; (b) Trend of cooling rate of the characteristic points.

The graphs in Figure 3 show the trend of the maximum temperatures and the cooling rates in the characteristic points analysed for each track. In terms of energy, the parameters of laser power and scanning speed have opposite effects on the thermal parameters. To simplify the analysis, a complex parameter comprising all of the previous, called energy density, was then calculated. As stated in the literature, it can be defined as following:

$$E_d = \frac{P}{vD} \quad (2)$$

The experimental plan reports two values of  $E_d$ : 36 J/mm<sup>2</sup> and 48 J/mm<sup>2</sup>. As shown in Figure 4, there is a positive correlation between energy density and  $T_{\max}$ , while the same parameter has a negative correlation with the cooling rate, the latter decreasing when the energy supplied to the substrate increases. The effect on maximum temperature is lower because it is affected by the opposite influence of powder. On the other hand, the cooling rate can be regarded as a superposition of the effects thus amplifying the general trend.

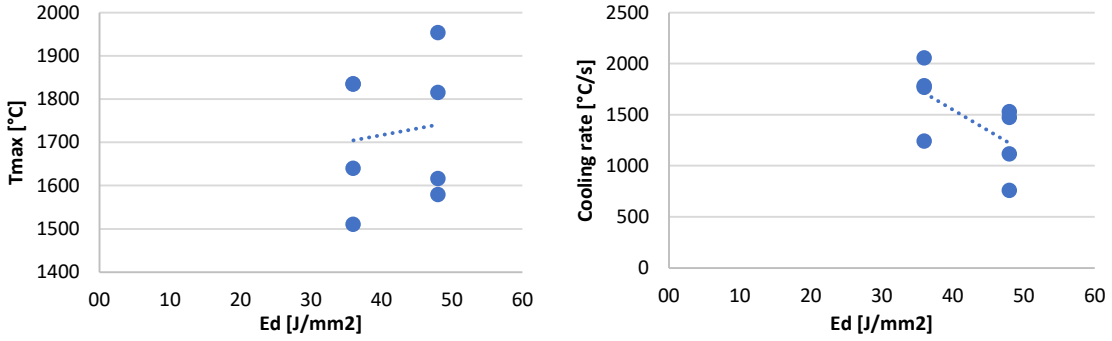


Fig. 4. (a) Maximum temperature vs energy density; (b) Cooling rate vs energy density.

### 3.2. Evaluation of geometrical characteristics

Through the geometrical analysis carried out by means of the microscope, we were able to obtain images that allowed us to measure width (W), height (H), depth (p), melt area (Amelt) and clad area (Aclad) of deposition. In fact, these measurements are indispensable for geometrical factors calculation and deposition quality definition, i.e. the dilution and the aspect ratio. The first parameter indicates the volumetric percentage of mixing between the clad material and the substrate. This parameter is calculated as the ratio between the areas of the molten substrate and area of the clad. An optimal value of this parameter should be around 10-30%, in order to assure bonding between the clad and the substrate, while preserving the homogeneity of the microstructure.

The aspect ratio is useful for evaluating the shape of the clad. An optimal range is set between 3 and 5 in order to avoid tracks with small material adding or large clads that could cause porosity issues. The AR is calculated as the ratio between the width and height of the clad.

$$\text{Dilution (area)} = \frac{A_{\text{melt}}}{A_{\text{melt}} + A_{\text{clad}}} \quad (3)$$

$$\text{Aspect ratio} = \frac{W}{H} \quad (4)$$

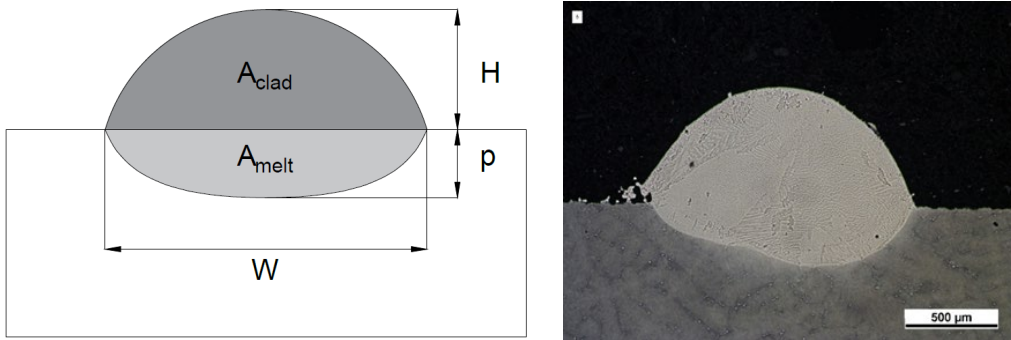


Fig. 5. (a) Schematic picture of clad deposition; (b) Cross-sectional morphology of sample 5

The table 2 shows all the calculated values of each single track:

Table 2 – Geometric characteristics of depositions

<i>N</i>	<i>W</i> [ $\mu\text{m}$ ]	<i>H</i> [ $\mu\text{m}$ ]	<i>p</i> [ $\mu\text{m}$ ]	<i>Aspect Ratio</i>	<i>A<sub>clad</sub></i> [ $\mu\text{m}^2$ ]	<i>A<sub>melt</sub></i> [ $\mu\text{m}^2$ ]	<i>Dilution (area)</i>
<b>1</b>	1485	194	461	7,65	187.872	519.773	73,5
<b>2</b>	1630	47	410	34,68	39.284	588.488	93,7
<b>3</b>	1958	188	479	10,41	235.583	615.187	72,3
<b>4</b>	1521	29	471	52,45	30.048	561.964	94,9
<b>5</b>	1430	642	320	2,23	689.263	320.291	31,7
<b>6</b>	1505	343	314	4,39	353.612	337.763	48,9
<b>7</b>	1393	1217	377	1,14	1.419.124	327.579	18,8
<b>8</b>	1440	650	216	2,22	699.012	230.994	24,8

In some cases, the dilution is very high (sample 1, 2, 3, 4). This is due to the low flow rates of powder, and also to an excessive heat transfer from the melting pool to the substrate. In fact, all these results are obtained for powder flow rates ranging from 1.5 to 2.5 g/min, which are too low for the laser energy density set for the experiments. For the considered range of flow rate, even the aspect ratio presented out-of-range values. The best geometrical configurations appear for high powder flow rates. The figure 5-b shows a cross section of samples 5.

### 3.3. Effects of thermal parameters on geometrical characteristics

In the previous analysis the fundamental thermal parameters (maximum temperature and cooling rate) have been plotted against the geometrical characteristics of the clad. Figure 6.a shows a remarkable correlation between the maximum temperature and the extension of the molten area. This is related to the thermal energy input that cause a variation of the surface temperature (read by the IR camera). An increase in energy density leads to a slower diffusion of heat through the base material. The temperature in the area below the laser spot will increase, bringing the material to melt and progressively increasing dilution. The slope of the regression line is therefore linked to the thermal properties of the base material. The minimum value is clearly identified by the melting temperature (1350°C), while the maximum value is related to the material vaporization temperature. By adopting high energy densities, the heat diffusion regime switches from conduction mode to keyhole mode, thus exponentially increasing the molten area [Campanelli et al., 2018]. Similarly, the cooling rate and the clad area are strictly related, due to heat accumulation in the clad region, which reduces the interface through which heat flux is transferred into the base material. In this way, the cooling rates that characterize the wider tracks are lower than those related to the narrow ones, thus affecting the clad microstructure. This phenomenon is amplified during the production of thin walls. The components have a minimal interface for the diffusion of heat and the pre-heating effects from the previous layers are superimposed, which substantially modifies the thermal cycles [Campanelli et al., 2018].



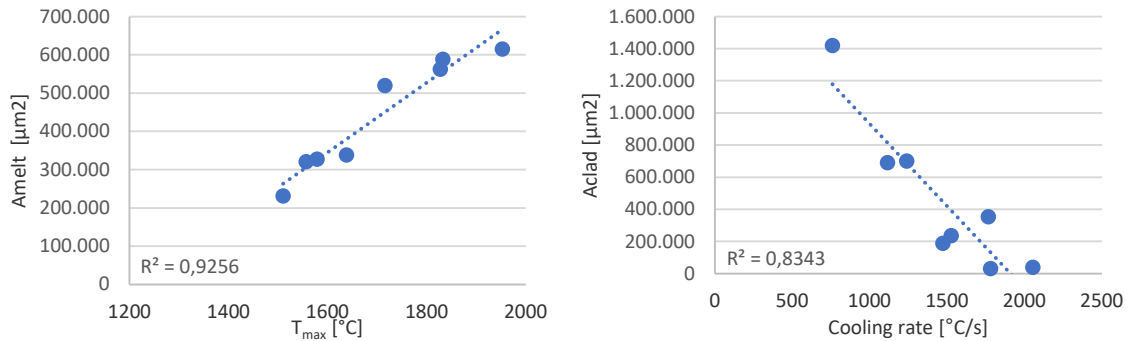


Fig. 6. (a) Melt area vs maximum temperature; (b) Clad area vs cooling rate

#### 4. Conclusion

In this work the effect of process parameters on thermal cycles, maximum temperature and cooling rate of single-track depositions of a Nickel-based superalloy on a substrate of the same material were studied. The monitoring of the temperature field of the DLMD process by means of an IR camera showed noticeable results and the following conclusions are drawn:

- the thermal parameters representing the temperature distribution on the samples are affected by a set of process parameters and the best way to predict them is analysing the density of energy;
- increasing the maximum cycle temperature leads to a widening of the molten area;
- the cooling rate and the microstructure are strongly affected by the clad area. In detail, a general increase of clad area leads to lower cooling rates and mechanical properties, associated to a thick grain microstructure.

#### References

- Wohlers, T., Gornet, T., 2014. History of additive manufacturing 34.
- Zhong, M., Liu, W., Ning, G., Yang, L., Chen, Y., 2004. Laser direct manufacturing of tungsten nickel collimation component. *J. Mater. Process. Technol.* 147, 167–173. <https://doi.org/10.1016/j.jmatprotec.2003.12.009>.
- Imran, M.K., Masood, S.H., Brandt, M., Bhattacharya, S., Mazumder, J., 2011. Direct metal deposition (DMD) of H13 tool steel on copper alloy substrate: Evaluation of mechanical properties. *Mater. Sci. Eng. A* 528, 3342–3349. <https://doi.org/10.1016/j.msea.2010.12.099>.
- Peng, L., Shengqin, J., Xiaoyan, Z., Qianwu, H., Weihao, X., 2007. Direct laser fabrication of thin-walled metal parts under open-loop control. *Int. J. Mach. Tools Manuf.* 47, 996–1002. <https://doi.org/10.1016/j.ijmachtools.2006.06.017>.
- Gao, W., Zhang, Y., Ramanujan, D., Ramani, K., Chen, Y., Williams, C.B., Wang, C.C.L., Shin, Y.C., Zhang, S., Zavattieri, P.D., 2015. The status, challenges, and future of additive manufacturing in engineering. *Comput.-Aided Des.* 69, 65–89. <https://doi.org/10.1016/j.cad.2015.04.001>.
- Angelastro, A., Campanelli, S.L., Casalino, G., Ludovico, A.D., Ferrara, S., 2011. A Methodology for Optimization of the Direct Laser Metal Deposition Process. *Key Eng. Mater.* 473, 75–82. <https://doi.org/10.4028/www.scientific.net/KEM.473.75>.
- Liu, W.-W., Tang, Z.-J., Liu, X.-Y., Wang, H.-J., Zhang, H.-C., 2017. A Review on In-situ Monitoring and Adaptive Control Technology for Laser Cladding Remanufacturing. *Procedia CIRP* 61, 235–240. <https://doi.org/10.1016/j.procir.2016.11.217>.
- Emamian, A., Farshidianfar, M.H., Khajepour, A., 2017. Thermal monitoring of microstructure and carbide morphology in direct metal deposition of Fe-Ti-C metal matrix composites. *J. Alloys Compd.* 710, 20–28. <https://doi.org/10.1016/j.jallcom.2017.03.207>.
- Farshidianfar, M.H., Khajepour, A., Gerlich, A., 2016a. Real-time control of microstructure in laser additive manufacturing. *Int. J. Adv. Manuf. Technol.* 82, 1173–1186. <https://doi.org/10.1007/s00170-015-7423-5>.
- Farshidianfar, M.H., Khajepour, A., Gerlich, A.P., 2016b. Effect of real-time cooling rate on microstructure in Laser Additive Manufacturing. *J. Mater. Process. Technol.* 231, 468–478. <https://doi.org/10.1016/j.jmatprotec.2016.01.017>.

- Muvvala, G., Patra Karmakar, D., Nath, A.K., 2017. Online monitoring of thermo-cycles and its correlation with microstructure in laser cladding of nickel based super alloy. *Opt. Lasers Eng.* 88, 139–152. <https://doi.org/10.1016/j.optlaseng.2016.08.005>.
- Campanelli, S.L., Angelastro, A., Latte, M., Rizzo, A., Palano, F., 2018. Thermal field monitoring and analysis of its influence on Direct Laser Deposition of single tracks of a nickel superalloy, in: Helvajian, H., Piqué, A., Gu, B. (Eds.), *Laser 3D Manufacturing V*. Presented at the Laser 3D Manufacturing V, SPIE, San Francisco, United States, p. 50. <https://doi.org/10.1117/12.2297667>.
- Song, L., Bagavath-Singh, V., Dutta, B., Mazumder, J., 2012. Control of melt pool temperature and deposition height during direct metal deposition process. *Int. J. Adv. Manuf. Technol.* 58, 247–256. <https://doi.org/10.1007/s00170-011-3395-2>.
- Ya, W., Pathiraj, B., Liu, S., 2016. 2D modelling of clad geometry and resulting thermal cycles during laser cladding. *J. Mater. Process. Technol.* 230, 217–232. <https://doi.org/10.1016/j.jmatprotec.2015.11.012>.